Asian Journal of Chemistry; Vol. 29, No. 7 (2017), 1612-1616

ASIAN JOURNAL OF CHEMISTRY

https://doi.org/10.14233/ajchem.2017.20616

Mesoporous COK-12 Supported Co_3O_4 Composites for Adsorption of Methylene Blue from Aqueous Solution

YADAGIRI JYOTHI[1,2], RESHMA[1], KONDEBOINA MURALI[2], B. SHANKAR[1], KAMARAJU SEETHA RAM RAO[2], BURRI DAVID RAJU[2] and PUPPALA VEERA SOMAIAH[1,*]

[1]Department of Chemistry, University College of Science, Osmania University, Hyderabad-500 007, India
[2]Catalysis Laboratory, CSIR-Indian Institute of Chemical Technology, Tarnaka, Hyderabad-500 007, India

*Corresponding author: Tel: +91 40 27682337; E-mail: vs_puppala@rediffmail.com; profvspuppala@gmail.com

Received: 1 March 2017; *Accepted*: 24 April 2017; *Published online*: 13 May 2017; AJC-18404

A simple batch adsorption experiment has been accomplished for the removal of methylene blue using Co_3O_4/COK-12 catalysts prepared by impregnation method with varying Co loadings (5-20 wt %). The as prepared catalysts were characterized by X-ray diffraction analysis, Fourier transform-infrared spectroscopy and nitrogen adsorption-desorption techniques to examine the morphology and the meso structure of the obtained composites. The effects of various experimental parameters, such as contact time, adsorbate dose, metal loading were investigated. Among the series 10 wt % Co_3O_4/COK-12 exhibited maximum adsorption capacity of about 27 mg/g. It was observed that the methylene blue adsorption represents pseudo-second order kinetics model as an appropriate model to represent the present data.

Keywords: Methylene blue, Co_3O_4/COK-12, Mesoporous structure, Amount adsorbed, Adsorption.

INTRODUCTION

Ever since the beginning of mankind, they have been trying to add colours to the world around them in various ways such as in textile, paper, leather tanning, plastics and food. During these processes the dye effluents are being dumped directly into the environment which constitutes a serious concern to the eco-system [1]. Hence it is important to remove the dyes from the effluents. The techniques generally employed for the removal of pollutants include adsorption, filtration, membrane separation [2-4], electrochemical destruction [5], ion-exchange and advanced oxidation technology [6]. Among these methods adsorption process is a highly efficient and low cost method with a simple operation process for waste water treatment [7-12].

Methylene blue (MB) is a cationic basic dye which is used in textile industries is hazardous and toxic on exposure to humans. The symptoms on exposure are increasing heart rate, vomiting, shock, Heinz body formation, cyanosis, jaundice, quadriplegia and tissue necrosis [13]. Further in aqueous solutions it is stable towards heat, oxidizing agents and non-degradable [14]. Due to these reasons methylene blue was chosen as a model compound for the adsorption studies.

Recently, numerous metal oxide nanoparticles have been used as adsorbents to remove methylene blue [15-22], but their main disadvantage is that they mainly exist in the colloidal form and very difficult to obtain spherical beads of the desired size for practical applications. Moreover, it is also very difficult to recover or separate MO_x nanoparticles from the solution after adsorption [23,24]. Suitable ways to circumvent this problem is to disperse the metal oxide particles onto supports with high surface area and loading MO_x nanoparticles in a polymer or resin [25,26]. The nanoparticles thus enhance the surface to volume ratio of the polymers and increase the available adsorption sites. These methods enhance the mechanical and chemical stability of the catalysts, which increase the practical utility and thermal reusability of the adsorbent.

Mesoporous material is one of the materials which offers possibility of preparing adsorbents that are applicable in many industrial processes by possessing high surface area, large adsorption capacity and porous structure making mesoporous materials as very promising candidates in oil refining, petro chemistry, organic synthesis and waste treatment [27-30]. Suraja *et al.* [31] reported the influence of SBA-15 support on Co_3O_4 catalyst for the adsorption of methylene blue. Hany *et al.* [32] reported the adsorption of methylene blue over Co_3O_4/SiO_2 catalysts. Warang *et al.* [33] reported for the photo degradation of methylene blue over Co_3O_4 catalysts synthesized by different techniques. Their disadvantage is that either the synthesis method or amount adsorbed is less. Recently,

COK-12 a simpler ordered mesoporous silica reported by Jammaer *et al.* [34] is a highly ordered 2D hexagonal mesoporous silica that is spontaneously formed at room temperature and at near neutral pH. Further this material has high surface area as well as ordered cylindrical channels with hexagonal arrangement with controllable pore size (about 6.9 nm) which is more than that of SBA-15 [34]. Due to these reasons we are interested to investigate the behaviour of COK-12 supported cobalt oxide materials in the adsorption of methylene blue dye for waste water treatment.

EXPERIMENTAL

Synthesis of materials: All the chemical reagents used in the experiments were obtained from commercial and used without further purification. The purity of p123 was 99 % and the purity of the inorganic precursors was not less than 99 %, respectively. Polymer template Pluronic P123, sodium silicate, citric acid, cobalt nitrate hexahydrate, methylene blue and sodium hydroxide were purchased from M/s Sigma Aldrich. Hydrochloric acid (35 wt %) was obtained from M/s Lobachemie, India.

Synthesis of COK-12: P6mm ordered mesoporous silica (COK-12) has been prepared by self-assembly method as reported by the Jammar *et al.* [34] using tri block copolymer pluronic P123 ($EO_{20}PO_{70}EO_{20}$, P123) as template and sodium silicate as SiO_2 source. In a typical synthesis, 4 g of the tri block copolymer pluronic P123 was dissolved in 107.5 mL of water. After a clear solution is obtained 3.684 g citric acid monohydrate and 2.54 g tri sodium citrate were added. The resulting surfactant solution was stirred for 24 h. To this surfactant solution 10.4 g sodium silicate solution diluted in 30 g of H_2O was added. The solution was stirred for 5 min at 400 rpm with a mechanical stirrer and kept at room temperature (293 K) without agitation for 24 h. The as-synthesized material was filtered, washed and finally dried at 333 K in hot oven for 12 h. Finally the materials was calcined for 8 h at 573 K and then for 8 h at 773 K with ramping of 1 K min^{-1} in flow of air.

Synthesis of Co_3O_4/COK-12 catalysts: COK-12 supported cobalt metal oxide catalysts were prepared by simple wet impregnation technique using $Co(NO_3)_2 \cdot 6H_2O$ as a cobalt oxide precursor. Briefly, requisite amount of precursor was dissolved in water and to this COK-12 was added. The mixture was allowed to complete dryness with occasional stirring on a hot plate. The dried solid was kept in a hot oven at 373 K for 12 h and then calcined in air at 723 K for 5 h with ramping of 10 K min^{-1}. The resultant solids were designated as xCC-12 where 'x' stands for Co_3O_4 weight percentage.

Characterization methods: Powder X-Ray diffraction (XRD) patterns were recorded on a Ultima IV diffractometer (M/s. Rigaku Corporation, Japan) with a Ni filter and Cu Kα radiation source (λ = 1.5406 Å) operated with a scan speed of 4° min^{-1} and a scan range of 0.7-80° at 40 kV and 20 mA. Surface area measurements were performed by N_2 physisorption on a Quadrasorb-SI (M/s. Quantachrome Instruments Corporation, USA). Prior to the measurement, the catalysts were degassed under vacuum (10^{-6} torr) at 423 K for 3 h to remove the physisorbed moisture. Surface areas were calculated using the Brunauer, Emmett and Teller (BET). Pore size distributions were calculated by using the Barret-Joyner-Halenda (BJH) method. UV-visible spectra were recorded on Shimadzu (160A), UV-Visible spectrophotometer using 1 cm quartz micro cuvettes (800-200 nm). The FT-IR spectra of the materials were recorded on GX spectrometer (M/s Perkin-Elmer, Germany) at ambient conditions using KBr discs.

Experimental methods: The adsorption of methylene blue was carried out by taking a stock solution of concentration 150 mg/L which is prepared by dissolving 150 mg of methylene blue in 1000 mL of water. In an experiment 50 mg Co_3O_4/COK-12 composite was added to 20 mL of stock solution under stirring and stirring was continued for a certain time (2-200 min) at room temperature. The solution was extracted and subsequently centrifuged at 2000 rpm for 10 min at different time intervals to separate Co_3O_4/COK-12 composite. The absorbance of the supernatant solution was estimated to determine the residual dye concentration with double beam spectrophotometer (HITACHI U 2000 spectrophotometer) before and after. The amount of adsorption at equilibrium, q_e (mg/g), was calculated by:

$$q_e = \frac{(C_0 - C_e)V}{W}$$

where C_0 and C_e (mg/L) are the liquid-phase concentrations of dye at initial and equilibrium, respectively. V is the volume of the solution (L) and W is the mass of dry adsorbent used (g).

RESULTS AND DISCUSSION

Fig. 1 illustrates the XRD patterns of COK-12 and xCC-12 catalysts prepared by a simple impregnation method. All the calcined catalysts in the low angle XRD patterns show three well resolved diffraction peaks corresponding to (100), (110) and (200) reflections identical to that of COK-12, indicating that the mesoporous structure of COK-12 is retained even after impregnating with the cobalt oxide but only with the slight decrease in the intensity of the reflections corresponding to (100). This decrease is due to the decreasing scatter contrast between pore walls and pore space [35].

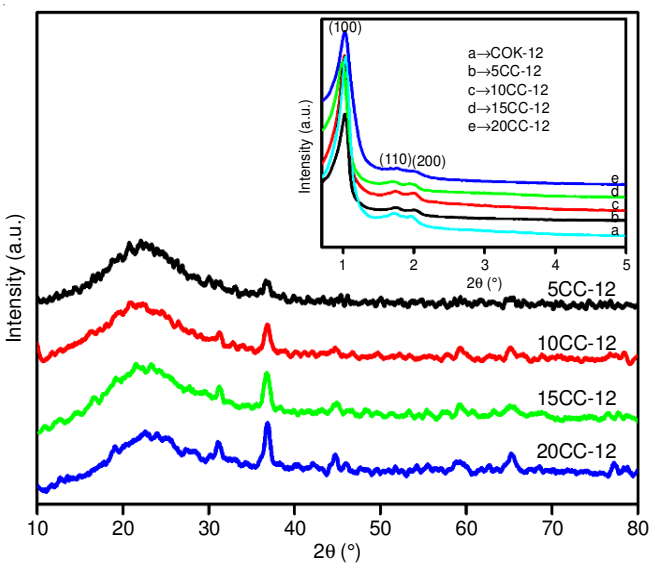

Fig. 1. XRD patterns of low and wide angle patterns of COK-12 and xCC-12 catalysts

A broad peak at 15° < 2θ < 30° in the wide-angle XRD patterns of all catalysts is consistent with the amorphous silica phase [36]. The wide angle XRD patterns of the catalysts with Co_3O_4 loadings show diffraction peaks corresponding to Co_3O_4 spinal (JCPDS No. 00-042-1467). The diffraction peaks at 2θ = 31.1°, 36.7°, 38.2°, 44.6°, 59.2° and 65.1° confirmed the crystallized spinal Co_3O_4 with space group Fd3m [37].

Fig. 2 shows the FT-IR spectra of the various loadings of cobalt oxide catalysts. The absorption bands at 1090, 807 and 473 cm^{-1} arise from the Si-O-Si stretching vibration. The absorption band at around 960 cm^{-1} can be assigned to either Si–OH or Si–O–Si stretching vibrations. The deformation modes of –OH bonds of adsorbed H_2O assigned at around 1630 cm^{-1} [37]. Finally the bands at around 662 and 562 cm^{-1} are assigned to Co-O stretching vibrations of the cobalt oxide spinal lattice of Co^{2+} and Co^{3+} ions [38,39]. The N_2 adsorption-desorption isotherms of COK-12 and various cobalt oxide loaded catalysts are displayed in Fig. 3. It can be seen that all the samples display type IV isotherm with H1 hysteresis loop characteristic of mesoporous COK-12 and are retained even after the deposition of cobalt oxide. At a lower relative pressure the decrease in the intensity of isotherms for cobalt oxide containing samples compared to the pure support COK-12 is due to decrease of the mean pore diameter after cobalt deposition. BET surface area and total pore volume has also been significantly decreased upon cobalt oxide impregnation and this tendency is greater at higher Co_3O_4 loadings. The BET surface area, pore volume and pore diameter are depicted in Table-1. The pore size distribution of catalysts (inset of Fig. 3) displays narrow pores within the range of 5-15 nm.

Effect of adsorbate concentration: The effect of adsorbate quantity of the dye using various amounts of methylene blue solution (25-125 mg/L/20mL) was studied using 0.05 g of 10CC-12 catalyst and the results are shown in Fig. 4. The equilibrium dye uptake capacity (q_e) was found to increase rapidly with an increase in the dosage of the adsorbate from 0 to 70 and then levelled off and was best when using 70 mg/L adsorbate. Thus, 70 mg/L of adsorbate was selected as the optimum adsorbate dosage. As the concentration is increasing

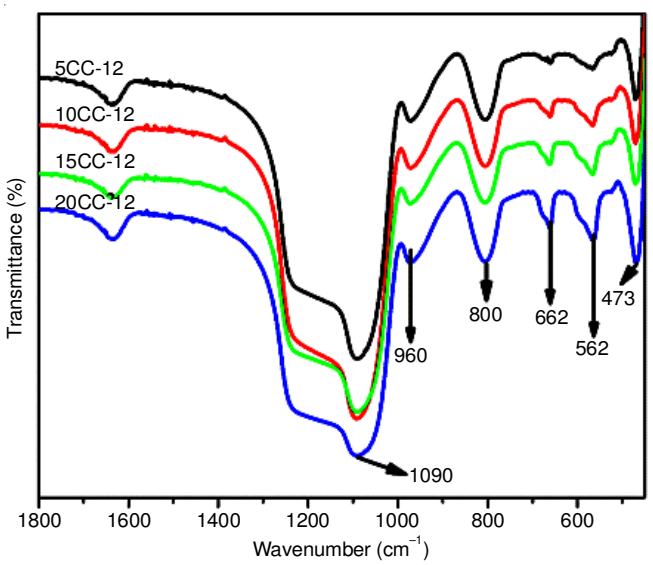

Fig. 2. FT-IR patterns of xCC-12 catalysts

TABLE-1
BET SURFACE AREA, TOTAL PORE VOLUME AND AVERAGE PORE DIAMETER OF COK-12 AND xCC-12 CATALYSTS

Co loading (wt %)	Co (ICP) loading (wt %)	BET surface area (m^2/g)	Total pore volume (mL/g)	Average pore diameter (nm)
COK-12	–	410	0.49	7.83
5CC-12	4.84	353	0.53	8.95
10CC-12	9.8	305	0.78	9.05
15CC-12	14.1	272	0.44	7.84
20CC-12	19.2	263	0.423	7.70

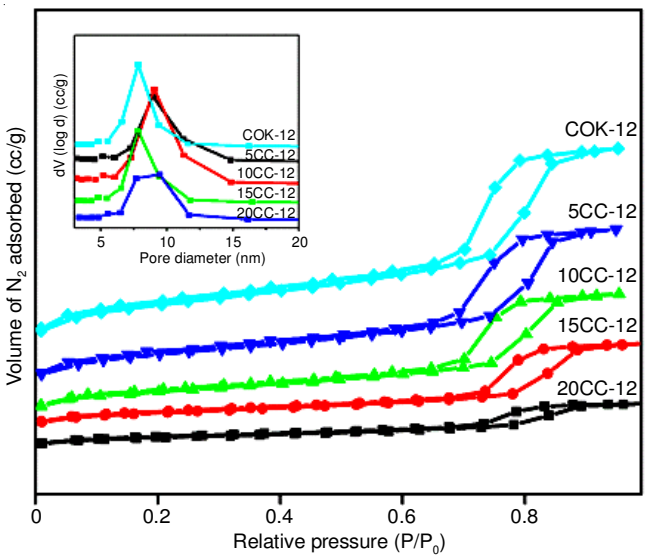

Fig. 3. N_2 adsorption-desorption isotherms of COK-12 and various cobalt oxide loaded catalysts

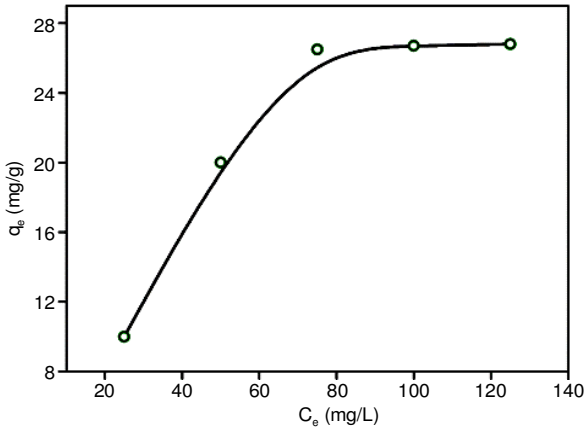

Fig. 4. Effect of adsorbate concentration on methylene blue adsorption. Reaction conditions: catalyst-0.05 g, methylene blue 20 mL/min, time - 150 min

from 10 to 70 mg/L the increase in the adsorption is due to increase in the driving force of the concentration gradient.

Effect of contact time: The effect of contact time on the adsorption capacity (q_t) is studied by varying contact time from 0 to 150 min for 70 mg/L of methylene blue concentration over 0.05 g of 10CC-12 catalyst and the results are shown in Fig. 5. Dye uptake increased rapidly for the first 30 min. This increase may be due to the diffusion of the dye molecules on to the adsorbent surface. After 30 min they proceeded at a slower rate and finally attained equilibrium at 60 min after which the amount of dye adsorbed was negligible. This may

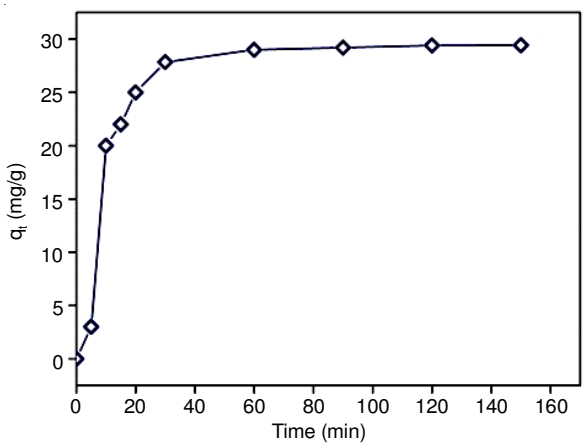

Fig. 5. Effect of contact time on methylene blue adsorption. Reaction conditions: catalyst-0.05 g, methylene blue 20 mL/min, Concentration of methylene blue 70 mg/L, time- 150 min

be due to the diffusion of the adsorbed molecules in to the porous structure of adsorbent. Hence the optimum time for the removal of the dye is taken as 60 min.

Effect of metal loading: Fig. 6 illustrates the effect of Co_3O_4 loading varying from 5 to 20 weight % on the adsorption capacity (q_t) for 70 mg/L for 60 min. The adsorption capacity (q_t) increases up to 10CC-12 and then levelled off. The increase in the adsorption is due to the increase in the number of active sites available for adsorption. Further on increasing the loading the amount adsorbed levelled off, this might be due to the decrease in the surface area and increase in the cobalt oxide loading.

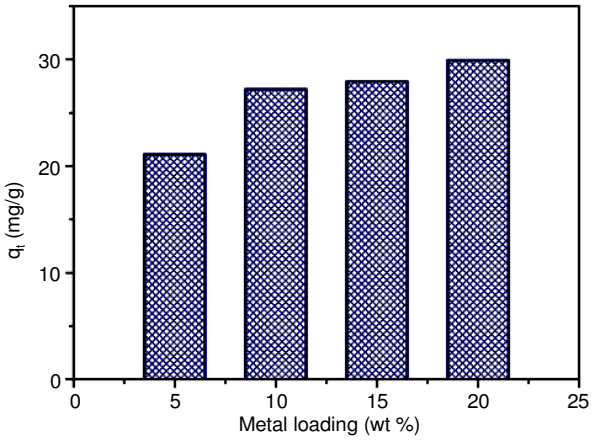

Fig. 6. Effect of Co_3O_4 loading on methylene blue adsorption. Reaction conditions: catalyst-0.05 g, methylene blue 20 mL/min, Concentration of methylene blue 70 mg/L, time-1 h

Adsorption kinetics: To examine the controlling mechanism for adsorption process Ho and McKay [40] have proposed the following equations to find out the pseudo-first-order and pseudo-second-order mechanisms.

$$\log (q_e - q_t) = \log q_e + \frac{k_1}{2.303} t \qquad (1)$$

From the slopes and intercepts of the plot log (q_e-q_t) *versus* t (Fig. 7) the first-order rate constant (k) and the amount adsorbed when the equilibrium (q_e) was reached can be evaluated and the obtained results using eqn. 1 are shown in Table-2. The correlation coefficients obtained for all samples using the first-order kinetic model were very high and q_e values deviated

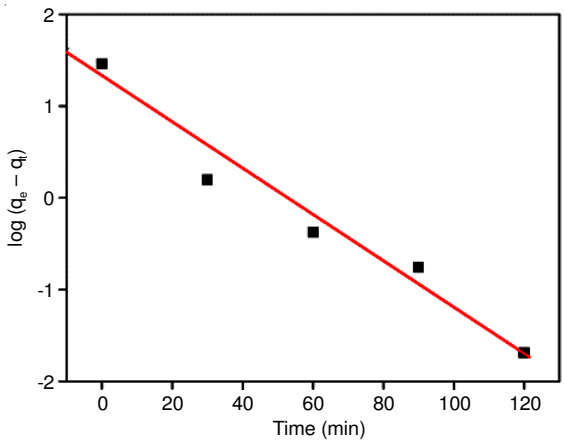

Fig. 7. First order kinetic model for batch adsorption of methylene blue

TABLE-2
KINETIC CONSTANTS OF METHYLENE BLUE ADSORPTION OVER 10CC-12 CATALYST

	k	q_e (mg/g)	Q_e(mg/g)
First order model	k_1 0.058	37.75	27
Second order model	k_2 0.027	28.7	27

k = Rate constant, k_1 (min^{-1}), k_2 (g mg^{-1} min^{-1}),
q_e = Amount adsorbed, Q_e = Amount adsorbed found

considerably from the experimental ones. These two observations indicated that the pseudo first-order equation might not be adequate to describe the mechanism for removal of methylene blue.

The linear pseudo second-order equation is given as follows [1]:

$$\frac{t}{q_t} = \frac{1}{k_2 q_e^2} + \frac{1}{q_e} t \qquad (2)$$

From the above equation second order rate constant, k can be evaluated from the intercept and the slope of the plot gives the value of q_e. Table-2 also lists the computed results obtained from the second-order rate equation. The computed results best fit the second order kinetic model and the value of q_e was close to the experimental, this indicate that the adsorption process here studied belong to a second order (Fig. 8). Table-3 presents the comparison of adsorption capacities of 10CC-12 catalyst with other mesoporous materials.

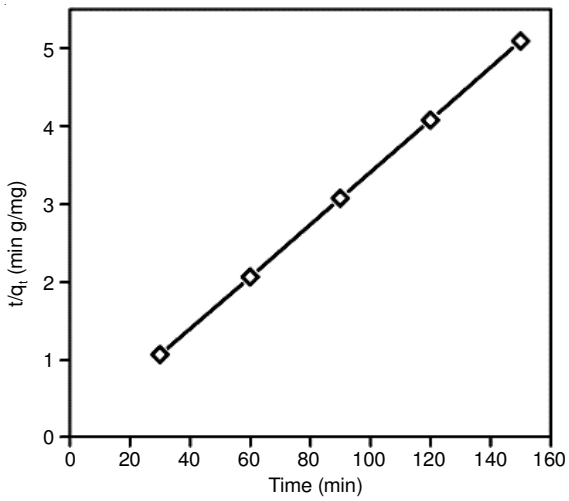

Fig. 8. Second order kinetic model for batch adsorption of methylene blue

TABLE-3
COMPARISON OF THE ADSORPTION CAPACITIES OF 10CC-12 CATALYST WITH OTHER MESOPOROUS MATERIALS

Catalyst	Amount adsorbed (mg/g)	Reference
SBA-15	10.44	[29]
10 Co_3O_4/SBA-15	16.66	[29]
Al-SBA-15	38.00	[30]
MCM-41	5.12	[29]
Ni-MCM-41	32.00	[29]
COK-12	10.32	Present study
10CC-12	27.00	Present study

Conclusion

Co_3O_4 doped COK-12 catalysts prepared by simple impregnation method were proved to be as an excellent material for the quantitative removal of methylene blue from aqueous solution with in no time of less than 30 min. The kinetics of methylene blue adsorption on to 10CC-12 followed the pseudo-second-ordermodel. These results indicated that the 10CC-12 could be employed as a low-cost material for the removal of methylene blue dye from wastewater.

ACKNOWLEDGEMENTS

The authors acknowledge to University Grants Commission and Council of Scientific and Industrial Research, New Delhi, India for financial support of this research.

REFERENCES

1. G.P. Anipsitakis, E. Stathatos and D.D. Dionysiou, *J. Phys. Chem. B*, **109**, 13052 (2005); https://doi.org/10.1021/jp052166y.
2. G.L. Dotto and L A A. Pinto, *J. Hazard. Mater.*, **187**, 164 (2011); https://doi.org/10.1016/j.jhazmat.2011.01.016.
3. S.J. Allen, G. Mckay and J.F. Porter, *J. Colloid Interface Sci.*, **280**, 322 (2004); https://doi.org/10.1016/j.jcis.2004.08.078.
4. Y. He, G. Li, H. Wang, J. Zhao, H. Su and Q. Huang, *J. Membr. Sci.*, **321**, 183 (2008); https://doi.org/10.1016/j.memsci.2008.04.056.
5. C.A. Martínez-Huitle and E. Brillas, *Appl. Catal. B*, **87**, 105 (2009); https://doi.org/10.1016/j.apcatb.2008.09.017.
6. S.H.S. Chan, T. Yeong Wu, J.C. Juan and C.Y. Teh, *J. Chem. Technol. Biotechnol.*, **86**, 1130 (2011); https://doi.org/10.1002/jctb.2636.
7. J.S. Mattson and H.B. Mark, Activated Carbon: Surface Chemistry and Adsorption from Solution, Marcel Dekker, New York (1971).
8. P.N. Cheremisinoff and F. Ellerbush, Carbon Adsorption Handbook Ann Arbor Science Publishers: Ann Arbor, MI (1979).
9. M.T. Uddin, M. Rukanuzzaman, M.M.R. Khan and M.A. Islam, *J. Environ. Manage.*, **90**, 3443 (2009); https://doi.org/10.1016/j.jenvman.2009.05.030.
10. S. Gupta and B.V. Babu, *J. Environ. Manage.*, **90**, 3013 (2009); https://doi.org/10.1016/j.jenvman.2009.04.006.
11. R. Gong, X. Zhang, H. Liu, Y. Sun and B. Liu, *Bioresour. Technol.*, **98**, 1319 (2007); https://doi.org/10.1016/j.biortech.2006.04.034.
12. V.K. Gupta and I. Ali, in ed.: A. Hubbard, Encyclopedia of Surface and Colloid Science; Marcel Dekker: New York, vol. 1, p. 136 (2002).
13. V. Vadivelan and K.V. Kumar, *J. Colloid Interface Sci.*, **286**, 90 (2005); https://doi.org/10.1016/j.jcis.2005.01.007.
14. Y. Xie, B. Yan, H. Xu, J. Chen, Q. Liu, Y. Deng and H. Zeng, *ACS Appl. Mater. Interfaces*, **6**, 8845 (2014); https://doi.org/10.1021/am501632f.
15. X.T. Zheng, X.Q. Ma and C.M. Li, *J. Colloid Interface Sci.*, **467**, 35 (2016); https://doi.org/10.1016/j.jcis.2015.12.052.
16. C. Pacurariu, O. Paska, R. Ianos and S.G. Muntean, *Clean Technol. Environ. Policy*, **18**, 705 (2016); https://doi.org/10.1007/s10098-015-1041-7.
17. H. Ma, J.B. Li, W.W. Liu, M. Miao, B.J. Cheng and S.W. Zhu, *Bioresour. Technol.*, **190**, 13 (2015); https://doi.org/10.1016/j.biortech.2015.04.048.
18. A. Ahmad, S.H. Setapar, C.S. Chuong, A. Khatoon, W.A. Wani, R. Kumar and M. Rafatullah, *RSC Adv.*, **5** 30801 (2015); https://doi.org/10.1039/C4RA16959J.
19. M. Vakili, M. Rafatullah, B. Salamatinia, A.Z. Abdullah, M.H. Ibrahim, K.B. Tan, Z. Gholami and P. Amouzgar, *Carbohydr. Polym.*, **113**, 115 (2014); https://doi.org/10.1016/j.carbpol.2014.07.007.
20. M. Rafatullah, O. Sulaiman, R. Hashim and A. Ahmad, *J. Hazard. Mater.*, **177**, 70 (2010); https://doi.org/10.1016/j.jhazmat.2009.12.047.
21. A. Ahmad, M. Rafatullah, O. Sulaiman, M.H. Ibrahim and R. Hashim, *J. Hazard. Mater.*, **170**, 357 (2009); https://doi.org/10.1016/j.jhazmat.2009.04.087.
22. L.W. Low, T.T. Teng, M. Rafatullah, N. Morad and B. Azahari, *Sep. Sci. Technol.* **48** 1688 (2013); https://doi.org/10.1080/01496395.2012.756912.
23. S. Abbasizadeh, A.R. Keshtkar and M.A. Mousavian, *Chem. Eng. J.*, **220**, 161 (2013); https://doi.org/10.1016/j.cej.2013.01.029.
24. D. Vu, Z. Li, H. Zhang, W. Wang, Z. Wang, X. Xu, B. Dong and C. Wang, *J. Colloid Interface Sci.*, **367**, 429 (2012); https://doi.org/10.1016/j.jcis.2011.09.088.
25. S. Abbasizadeh, A.R. Keshtkar and M.A. Mousavian, *J. Ind. Eng. Chem.*, **20**, 1656 (2014); https://doi.org/10.1016/j.jiec.2013.08.013.
26. H. Mittal, A. Maity and S.S. Ray, *Chem. Eng. J.*, **279**, 166 (2015); https://doi.org/10.1016/j.cej.2015.05.002.
27. A. Corma, *Chem. Rev.*, **97**, 2373 (1997); https://doi.org/10.1021/cr960406n.
28. A. De Stefanis, S. Kaciulis and L. Pandolfi, *Micropor. Mesopor. Mater.*, **99**, 40 (2007); https://doi.org/10.1016/j.micromeso.2006.08.033.
29. Y. Shu, Y. Shao, X. Wei, X. Wang, Q. Sun, Q. Zhang and L. Li, *Micropor. Mesopor. Mater.*, **214**, 88 (2015); https://doi.org/10.1016/j.micromeso.2015.05.006.
30. Z. Wu, Q. Lu, W.H. Fu, S. Wang, C. Liu, N. Xu, D. Wang, Y.M. Wang and Z. Chen, *New J. Chem.*, **39**, 985 (2015); https://doi.org/10.1039/C4NJ01473A.
31. P.V. Suraja, Z. Yaakob, N.N. Binitha, S. Triwahyono and P.P. Silija, *Clean Technol. Environ. Policy*, **15**, 967 (2013); https://doi.org/10.1007/s10098-012-0558-2.
32. H.H. Abdel Ghafar, G.A.M. Ali, O.A. Fouad and S.A. Makhlouf, *Desalin. Water Treat.*, **53**, 2980 (2015); https://doi.org/10.1080/19443994.2013.871343.
33. T. Warang, N. Patel, R. Fernandes, N. Bazzanella and A. Miotello, *Appl. Catal. B*, **132-133**, 204 (2013); https://doi.org/10.1016/j.apcatb.2012.11.040.
34. J. Jammaer, A. Aerts, J. D'Haen, J.W. Seo and J.A. Martens, *J. Mater. Chem.*, **19**, 8290 (2009); https://doi.org/10.1039/b915273c.
35. J. Wang and Q. Liu, *Micropor. Mesopor. Mater.*, **83**, 225 (2005); https://doi.org/10.1016/j.micromeso.2005.04.012.
36. O. Gonzalez, H. Perez, P. Navarro, L.C. Almeida, J.G. Pacheco and M. Montes, *Catal. Today*, **148**, 140 (2009); https://doi.org/10.1016/j.cattod.2009.03.030.
37. J. Taghavimoghaddam, G.P. Knowles and A.L. Chaffee, *J. Mol. Catal. Chem.*, **358**, 79 (2012); https://doi.org/10.1016/j.molcata.2012.02.014.
38. T. Tsoncheva, L. Ivanova, C. Minchev and M. Froba, *J. Colloid Interface Sci.*, **333**, 277 (2009); https://doi.org/10.1016/j.jcis.2008.12.070.
39. P. Visuvamithiran, B. Sundaravel, M. Palanichamy and V. Murugesan, *J. Nanosci. Nanotechnol.*, **13**, 2528 (2013); https://doi.org/10.1166/jnn.2013.7388.
40. Y.S Ho and G McKay, *Process Biochem.*, **34**, 451 (1999); https://doi.org/10.1016/S0032-9592(98)00112-5.